Transactions of The Indian Institute of Metals
Vol. 62, Issue 3, June 2009, pp. 197-208

Use of wear mechanism map to engineer surfaces for enhanced wear resistance

Manish Roy

Defence Metallurgical Research Laboratory, PO: Kanchanbagh, Hyderabad-500 058, India

E-mail : rmanish64@rediffmail.com

Received 02 May 2008
Revised 16 February 2009
Accepted 20 March 2009
Online at www.springerlink.com

Keywords:
sliding wear; wear mechanisms; surface engineering; coatings

Abstract

Material degradation due to unidirectional sliding wear can be found in wide range of engineering applications. Depending on the applied load and sliding velocity, several material removal mechanisms will be operative during sliding. Lim and Ashby compile these mechanisms in the form of wear mechanism map. They have also been able to estimate the wear rate in each mechanism quantitatively. However, no effort has hitherto been made to use these expressions and concepts to alter or modify the surfaces of various materials for improved wear performances. The objective of the present work is to address this issue. In this work, the expression for wear rate in various regimes will be examined critically. The important parameters that governs wear rate will be identified. An approach to improve wear rate in each regime will be suggested on the basis of identified parameters. Suggestions will be substantiated with large database and published work.

1. Introduction

The engineering problem of wear is known even in ancient time. The development of understanding in wear over past few decades has been phenomenal. A variety of modes of wear such as sliding wear, erosive wear, abrasive wear, etc., have been identified. Even in each mode of wear, a large number of material removal mechanisms are being reported. During sliding wear, several mechanism of material removal can be envisaged depending on sliding velocity and applied load. These mechanisms are put together in the form of a map by Lim and Ashby [1]. Several other maps have subsequently been reported [2-4]. Further, Lim and Ashby have also been able to estimate the wear rate in each mechanism quantitatively. In present days, modification of surfaces without altering the bulk properties of various components has become an area of intense research activities. However, no effort has hitherto been made to modify or alter the surfaces of engineering components using the expression and concepts suggested by Lim and Ashby [1]. This paper presents the design consideration to modify the surfaces of engineering components for tribological application in the light of wear mechanism map. In the last few years several reviews have been made in design and developments of hard coating for tribological application [5-8]. But approach in this direction is not yet reported. The design consideration introduced in this work is also exemplified with appropriate research results. These results can also modify the boundaries of Wear map as identified by Lim and Ashby [1].

2. Design consideration for various wear modes

In this part various wear modes along with the expression for wear rate will be described. These modes, compiled by Lim and Ashby [1] in the form of wear mechanism map, are shown in Fig. 1. The method to improve the wear rate will be discussed in the light of results available in the literature.

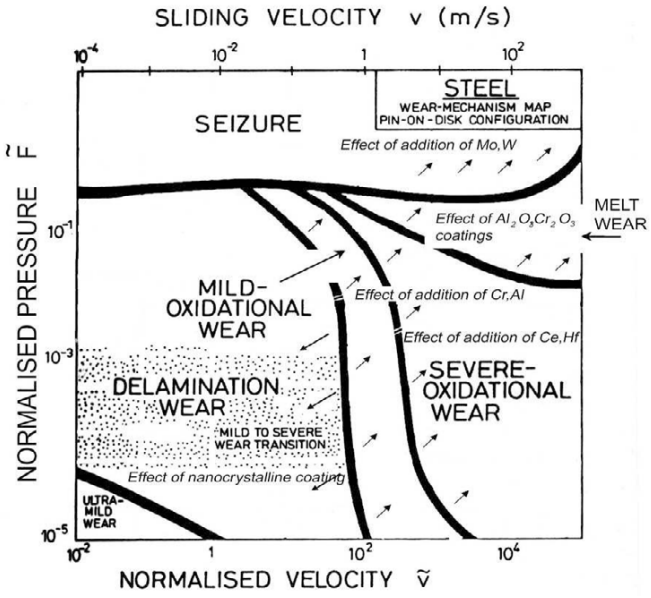

Fig. 1 : The wear mechanism map.

2.1 Plasticity dominated wear

This mode of wear prevails at relatively low load and low sliding velocity. Wear in this regime is governed by the deformation behaviour of the wearing material. Material loss is primarily by delamination. The wear rate (W) in this regime is given by,

$$W = k\frac{F}{H} \quad (1)$$

where k is known as wear coefficient, F is applied load and H is hardness of wearing material.

The wear rate in this regime can be reduced by modifying the surface of a component with a layer having

i) Low wear coefficient k, or
ii) High hardness H

Table 1 and Table 2 give the value of wear coefficient k [9], whereas hardness of large number of potential wear resistant materials is listed in Table 3 [10]. It can be seen from Table 1 that WC has got minimum wear coefficient. It is even less when WC slides against mild steel. This is why WC-Co coating has become most widely used coating for protection against sliding wear. This coating can be deposited primarily by thermal spraying [11-15]. However, other methods of deposition such as physical vapor deposition (PVD), chemical vapor deposition (CVD), cathodic arc etc., are also demonstrated [15-17]. Excellent tribological performances of WC-Co coating are reported in literature [18-20]. Figure 2 due to Roy *et al*. [15] indicated significant improvement of wear resistance of WC-Co coating on mild steel on depositing WC-Co coating by thermal spraying under reciprocating condition at applied load of 2, 5 and 10 Kg for stroke length of 12.5 mm.

Table 1 : Wear coefficient table for self-mating materials

Combination	*Wear coefficient x 10^4*
Iron on iron	9.0
Iron on white metal	1.2
Low carbon steel on low carbon steel	70
Cadmium on Cadmium	57
Zinc on Zinc	530
Silver on Silver	40
Copper on Copper	110
Platinum on Platinum	130
Mild steel on mild steel	150
Stainless steel on Stainless steel	70
Tool steel on Tool steel	1.3
Tungsten carbide on Tungsten carbide	0.01

Table 2 : Wear coefficient table for different mating materials

Combination	*Wear coefficient*
60/40 brass on tool steel	6
70/30 brass on tool steel	1.7
Silver steel on tool steel	0.6
Beryllium copper on tool steel	0.37
Stellite on tool steel	0.55
Ferritic stainless steel on tool steel	0.17
Tungsten carbide on low carbon steel	0.04

Table 3 : Hardness (VHN) of typical hard coat materials

Element	*Carbide*	*Nitride*	*Boride*
Boron	3700	4500	
Chromium	1600-Cr_2C_3	2200	1800
Hafnium	2270-2650	1640	2250-2900
Molybdenum	1800-MoC		2350
Niobium	2400-2850	1396-NSN	
Silicon	3500		
Tantalum	1800-2450	1220	2450-2910
Titanium	2000-3200	1200-2000	2200-3500
Tungsten	2100-2400		2400-2660
Vanadium	2460-3150		2070-2800
Zirconium	2360-2600		2250-2600

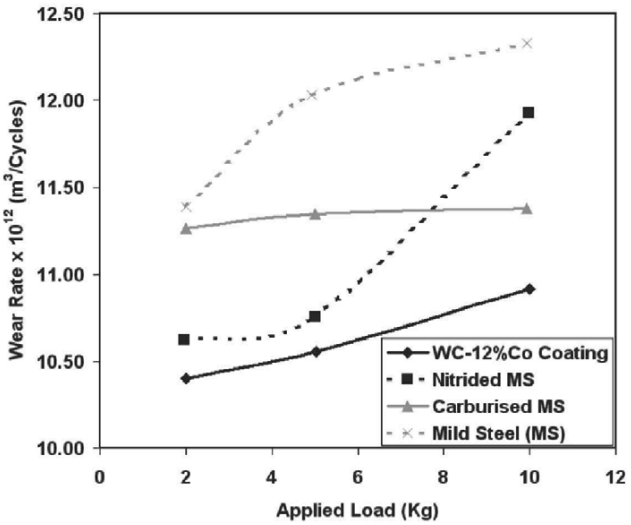

Fig. 2 : Improvement of wear resistance of mild steel by thermal spraying of WD-12% Co coating [15].

Perusal of Table 3 indicates very high hardness of cubic boron nitrite (C-BN) coating. In fact, the hardness of this coating is second to diamond. Such high hardness of C-BN coating along with its high thermal and chemical stability makes it extremely sought after coating for tribological application. C-BN coatings can be deposited by PVD techniques only [21]. Coatings deposited by CVD are hexagonal and have much lower hardness. These hexagonal boron nitride coatings are not used for tribological applications [22]. Because of high hardness, a large number of coatings such as polycrystalline diamond (PCD), diamond like carbon (DLC), hard carbon, etc., are considered viable option in present days. Most of the hard coatings are nitrides (TiN, CrN etc.), carbides (TiC, CrC, WC/C etc.), oxides (Al_2O_3, Cr_2O_3 etc.) or combination of these coatings. Though these hard coatings exhibit good wear resistance, they are essentially high friction coatings and their friction levels vary in-between 0.4 to 0.9 in dry sliding [6]. In contrast, coatings such as MoS_2, DLC can be classified as low friction coatings with friction coefficient typically in between 0.05 to

0.25 in dry sliding [23,24]. Poly crystalline diamond coating (PCD) obtained by CVD exhibits high hardness and wear resistance along with low friction coefficient. This makes diamond coating suitable for very demanding application [25].

While engineering the surface of a material for improved performances, attention should be paid in the bulk temperature of the wearing surface. This bulk temperature (T_b) is given as,

$$T_b = T_0 + \frac{\alpha \mu F v l_b}{A_n K_m} \quad (2)$$

Where T_o is room temperature, α is a constant known as heat distribution coefficient, μ is the friction coefficient, F is applied load, v is sliding velocity, l_b is mean heat diffusion distance, A_n is nominal area of contact and K_m is thermal conductivity of the metal. If T_b is high, the hardness of the hardened layer tends to come down. One-way of reducing the temperature is to lower the friction coefficient. On a sliding surface, for a given sliding velocity, the friction coefficient depends on the crystal structure of the surface. The crystal structure will determine the number of slip system available. If the number of slip system is high, μ and hence T_b will be low. This, in turn will reduce the tendency to soften.

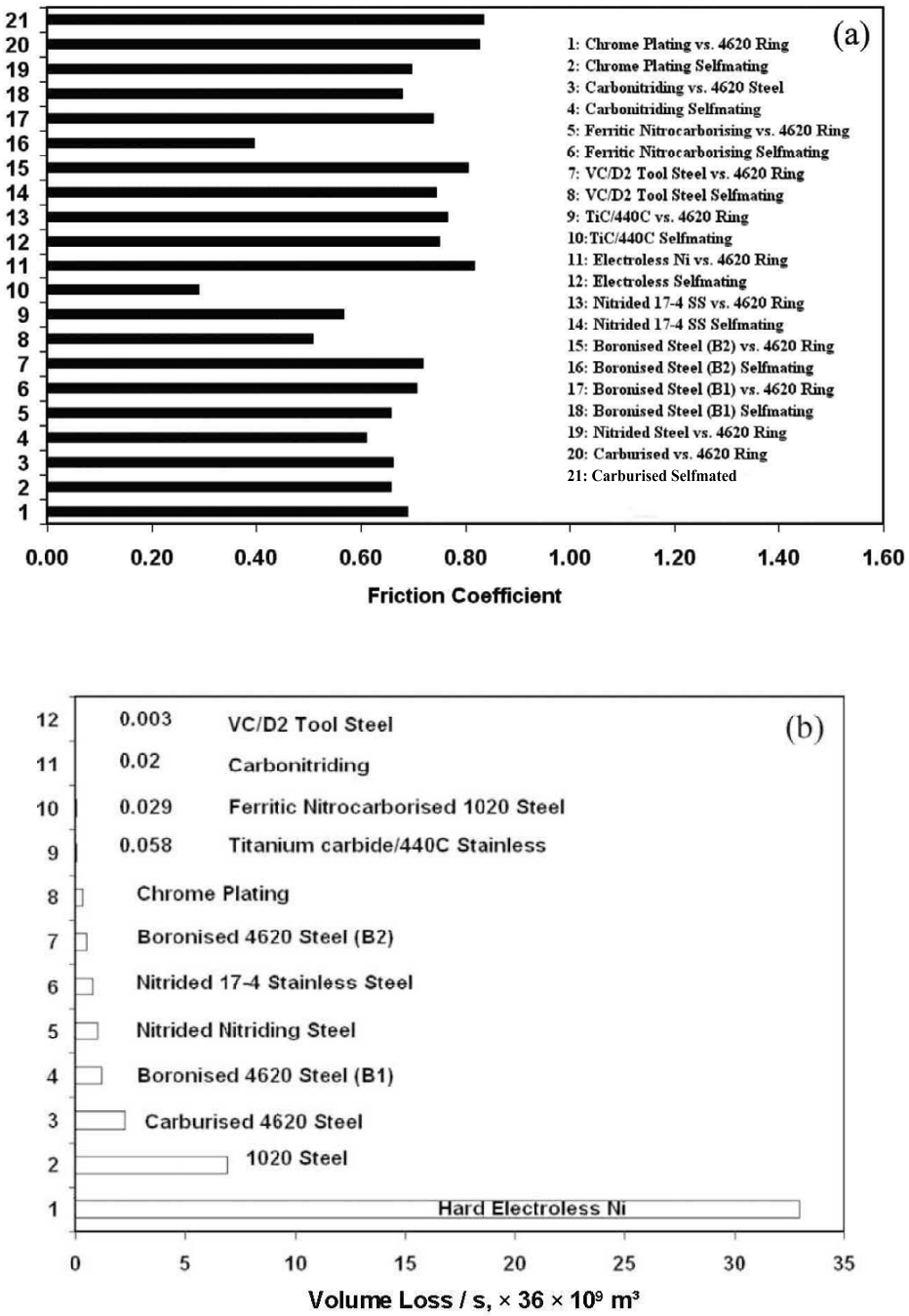

Fig. 3 : The bar diagram showing the (a) friction coefficient and (b) the wear rate of various diffusion treated surfaces [28].

To illustrate an example where such principle can be applied advantageously is carburising and nitriding. In both the cases, wear resistance is improved by hardening the surface of the component. In carburising hardening is achieved by transforming the carbon rich austenite into martensite, which has BCT structure. In contrast, nitriding is done on ferritic matrix having BCC structure. The available slip system in BCC nitrided layer is higher than BCT curburised layer giving rise to low friction and less increase of temperature. Consequently nitrided layer does not get softened due to raise of temperature even at relatively harsh environment. The work due to Krishnaraj *et al.* [26] clearly confirms the above statement. They noted superior performances of nitrocarburizing to martensite hardening for hot working die application. On the contrary, Rizvi and Khan [27] found opposite results with H13 tool steel which was gas alloyed by tunsten arc. The higher wear resistance of carburised layer compared to nitrided layer was attributed to formation of fine dendrite microstructure containing Chromium – Vanadium carbides.

An alternate approach is to put a layer, which does not soften, even at relatively high temperature. For example, boronised layer can retain its wear resistant properties at a higher operating temperature compared to carburised layer [28,29]. The observation of Budinsky [28] is given in Fig. 3, where bar diagram exhibits the friction coefficient (Fig. 3a) and wear rate (Fig. 3b) for a series of diffusion treated and electroplated steel. He carried out test using block on ring at a load of 45 N, rotating speed of 10.5 rad/s for two hours corresponding to sliding distance of 4323 m. The above experimental condition is valid for Fig. 3a whereas the experiment pertaining to Fig. 3b was done using loop abrasion tester at a load of 200 gm, at a sliding speed of 0.28 m/s for a total sliding distance of 914 m. Lower friction coefficient of the nitrided layer leading to low wear rate compared to carburised layer can be seen. It also exhibits lower friction coefficient and lower wear rate of the boronised layer than the carburised layer. This superior wear properties may not be realised for a boronised layer obtained through conventional route as conventional boronising is carried out at higher temperature for long time affecting bulk properties of the component and it forms a brittle boronised layer containing several phases [29]. Consequently, ion boronising or laser boronising is recommended [30,31].

Going back to equation (1) it can be stated that hardness of most of the annealed material is directly related with their melting temperature [32]. In other words, wear rate of a material can be reduced if the surface is alloyed with high melting materials. Using this concept, the performance of Al alloy (6061) subjected to wear is improved by alloying the surface with high melting Ni-20Cr alloy [33]. These results are shown in Fig. 4. In this work laser surface alloyed Al alloy was subjected to fretting action under a ball on flat configuration at ambient condition, at relative humidity of 50 %. The frequency of test, applied load and amplitude of reciprocation were 50 Hz, 2 N to 5 N and 50 to 100 μm respectively. Figure 4 shows the variation of wear rate with total number of cycles for different testing conditions. In all the cases wear rate of laser alloyed Al 6061 is lower than the substrate. Further analysis of this work is carried out in subsequent section 3.0.

In recent times a large number of thin coatings have exhibited their potential for wear resistance application. These hard coatings fail at the interface of the substrate due to strain mismatch during tribological degradation. This

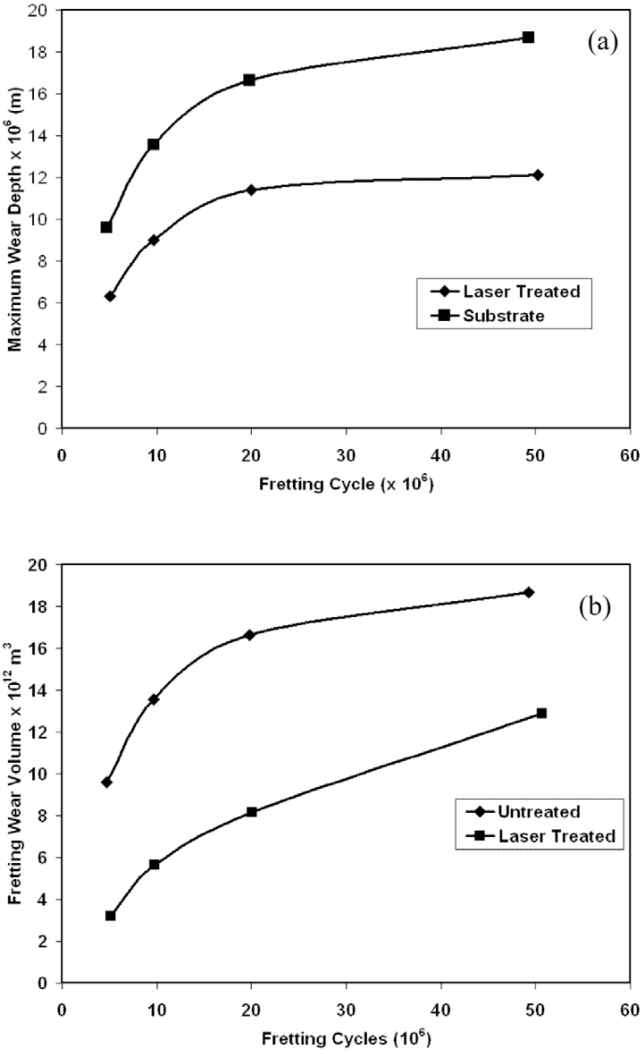

Fig. 4 : The influence of total number of cycles on the wear rate of the laser surface alloyed aluminum substrate [33].

phenomenon has given rise to development of duplex coatings. Nitriding to get hardened layer followed by PVD coating on steel and titanium alloy has given better results [34-36]

Nanocrystalline materials are well known for improved hardness, yield strength and toughness. In recent times enhanced tribological performances of nano crystalline thin and thick coatings are reported [37,38]. The investigation of Wang *et al*. [38] is given in Fig. 5. In Fig. 5 the variation of the wear volume with time is presented for Al_2O_3 / TiO_2 coating with conventional grain size and three different Al_2O_3 / TiO_2coatings with nano crystalline grain size. The test was conducted using a polishing and grinding machine at an applied load of 90 N and sliding velocity of 2.67 m/s. Lower wear rate of nanocrystalline coating is evident. In another study by Roy *et al*. [39], nanocrystalline Cr_3C_2-25(Ni20Cr) coating exhibited 25% lower friction coefficient compared to similar coating with conventional grains. In this work, Cr_3C_2-25(Ni20Cr) coated 253 MA alloy was subjected to sliding wear at a load of 70 N, sliding speed of 0.25 m/s. This behaviour is shown in Fig. 6. Several coatings exhibited better performances by doping with insterstitial e.g. a distinctly harder and more wear resistant Ti(B)N top coat compared with pure PVD TiN [40] is reported. Similar observation is made for Tungsten (doped with carbon) [41] and for Chromium (doped with nitrogen) [42].

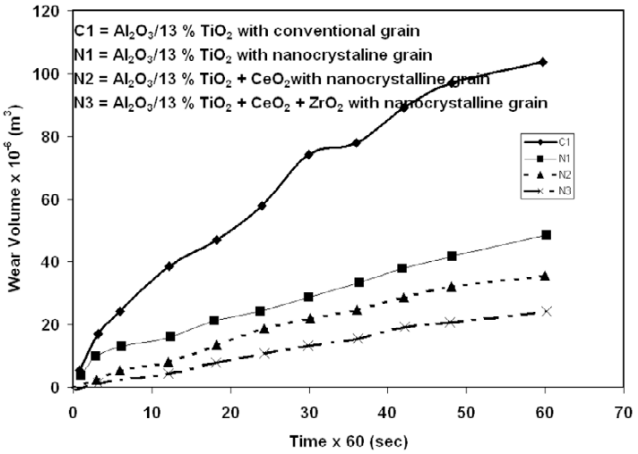

Fig. 5 : The variation of wear rate of various nanocomposite coatings as function of time [38]. (C1): Al_2O_3 +13 % TiO_2 with conventional grain, (N1): Al_2O_3 +13 % TiO_2 with nanocrystalline grain, (N2): Al_2O_3 +13 % TiO_2 + CeO_2 with nanocrystalline grain and (N3): Al_2O_3 +13 % TiO_2 + CeO_2 + ZrO_2 with nanocrystalline grain.

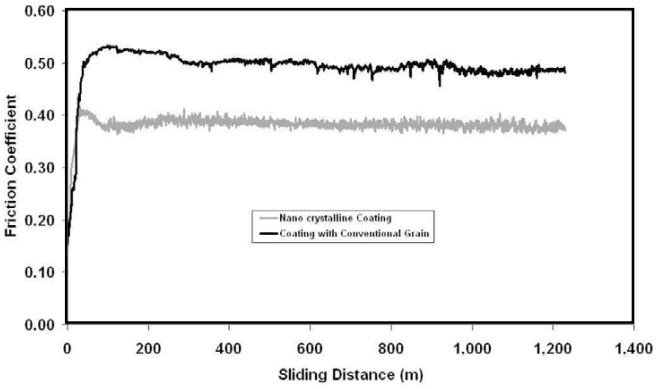

Fig. 6 : The variation of friction coefficient as function of sliding distance for Cr_3C_2-25(Ni20Cr) coating with nanocrystalline grains and with conventional grains [48].

2.2 Mild oxidational wear

At an intermediate sliding speed and applied load, mild oxidational wear becomes prevalent. The wear rate (W) for mild oxidation is given as,

$$W = \frac{FC^2A_o}{vZ_cH_0}\exp\left(-\frac{Q}{RT_f}\right) \quad (3)$$

where A_o is Arrhenius constant, Q is the activation energy for oxidation, Z_c is the critical thickness of spalling, T_f is the temperature at the place of contact of the asperities, v is the sliding velocities, C is a constant which depends on the composition of the oxide scale and R is the molar gas constant.

The temperature at the place of contact of the asperities, known as flash-heating temperature is given by

$$T_f = T_b + \frac{\mu v r}{2K_e}\left(\frac{H_oF}{NA_n}\right)^{\frac{1}{2}} \quad (4)$$

Where H_o is the hardness of the oxide scale, N is the total no of the asperities, r is the radius of the contacting area and K_e is the equivalent thermal conductivity. Other symbols have their meaning described previously.

Thus, the wear rate in this regime can be reduced by,

1. Reducing Arrhenious constant A_o
2. Increasing activation energy for oxidation Q, and
3. Increasing critical thickness for spalling (Z_c)

The oxidation under sliding wear takes place at a rate higher than that observed under static condition [43-45]. The observed difference comes due to change of Arrhenious Constant A_o, which again depends on material and wearing condition [46]. However, activation energy for oxidation Q remains unchanged [47]. Hence, further discussion on lowering wear rate will be confined on activation energy Q and critical thickness of spalling (Z_c).

The activation energy for oxidation (Q) for a large number of oxide scale are compiled in Table 4[48]. According to Table 4, activation energy for oxidation are on the higher side for Al_2O_3 and Cr_2O_3 scale formation. Hence, many surface engineering for wear resistant in this regime involves forming of Al high or Cr high layer formation. This can be achieved by,

1. Alloying the surface with Al or Cr by laser.
2. Aluminizing or chromising by diffusion coating or CVD
3. Increasing Al, Cr concentration near surfaces by plasma ion treatment or ion implantation.
4. Depositing Al_2O_3 or Cr_2O_3 layer directly by thermal spraying.

Hirose *et al.* [49] found improved wear performance on alloying Ti with Al by laser surface alloying. Ti when undergoes mild oxidation wear TiO_2 forms. This layer forms and grows at very high rate and wears out by spalling. When alloyed with Al by laser surface alloying, protective Al_2O_3 scale forms. Since activation energy for formation of Al_2O_3 is much higher compared to TiO_2, scale growth of this oxide scale is much slower. Thus it takes long time for the critical spalling thickness to be attained leading to reduced wear rate.

Similarly, Tau and Doong [50] found chromium alloyed surface exhibiting higher wear resistance compared to untreated steel for a given hardness and structure. This behaviour can also be attributed to the fact that chromium rich layer forms Cr_2O_3 scale which exhibits better adhesion to the substrate than Fe_2O_3 scale that forms on untreated

Table 4 : Activation energies for anion and cataion diffusion of various oxides

Oxide scale	*Activation energy for Cataion diffusion (Cal/mol)*	*Activation energy for Anion Diffusion (Cal/mol)*
NiO	54000	45900
CoO	36000	34500
CuO	39300	36100
ZnO	16500	45300
Cr_2O_3	—	61100
Al_2O_3	57600	114000
SiO_2	29000	79000

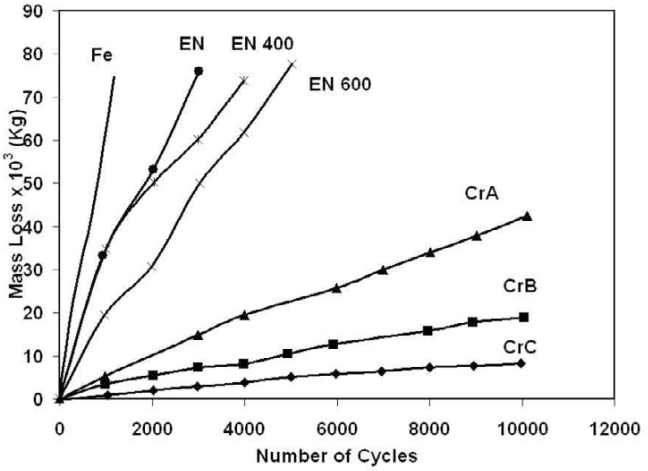

Fig. 7 : The variation of mass loss as function of total no of cycles for chromium and nickel coated steel [51].

steel. Gawne and U.MA [51] also reported improved wear performances of stainless steel coated with Cr and Ni when tested at 200 kgf load for rotating sped of 1 rev /s. Their observation is illustrated in Fig. 7 where mass loss of uncoated steel and several varieties of Ni and Cr coating is plotted against number of cycles. In this figure Fe, En, En 400 and En 600 represent substrate, electroless Ni plating, electroless Ni plating heat treated at 400°C and electroless Ni plating heat treated at 600°C respectively. In contrast, CrA, CrB and CrC correspond to different electrolytic Cr platings deposited using conventional sulphate ion catalysed chromic acid, high speed mixed catalysed solution and modified high speed mixed catalysed solution respectively. As can be seen from Fig. 7 that Cr coating exhibit less wear rate than Ni coating and Ni coating has less wear rate than the substrate. This can be attributed to the fact that Cr coating forms Cr_2O_3 scale and Ni coating forms NiO scales during wear. The activation energy for formation of Cr_2O_3 scale is much higher than the activation energy of formation of NiO scale. This will cause Cr coating to take longer time to get Cr_2O_3 scale of critical thickness for spalling than the time taken by Ni coating to get NiO scale of critical thickness. Thus Cr coating can undergo wear for longer time than Ni coating with less wear rate. This is in spite of the fact that NiO scale has excellent adhesion to Ni substrate during isothermal oxidation. That is why Cr coating exhibit less wear rate.

Table 5: Oxide metal volume ratio for aome common metals

S.No.	*Oxide scale*	*Oxide-metal volume ratio*
1	MgO	0.81
2	Al_2O_3	1.28
3	ZrO_2	1.56
4	Cr_2O	1.64
5	NiO	1.65
6	FeO	1.68
7	TiO_2	1.70-1.78
8	CoO	1.86
9	Cr_2O_3	2.07
10	Fe_3O_4	2.10

The third method of bringing down the wear rate is to increase the critical thickness of spalling. Spalling takes place due to generation of.

1) Growth stress [52]
2) Thermal stress [53]

Growth stress is due to

i) Epitaxial stress [54]
ii) Compositional changes in alloys or scales [55]
iii) Point defect stresses [56]
iv) Specimen geometry
v) Volume differences between the oxide and the metal from which it forms

This volume difference between the oxide scale and the metal is controlled by Pilling Bedworth [57] ratio as,

$$PBR = \frac{V\,(per\ metal\ ion\ in\ oxide)}{V\,(per\ metal\ atom\ in\ metal)}$$

The PBR ratios for some common metals are given in Table 5 [48]. As the PBR ratio is closer to 1, residual stresses will be less and adhesion of the scale will increase. Thus, from Table 5, Al_2O_3 is the most potential scale with minimum PBR ratio after MgO. However, MgO is not used as protective coating due to other problems such as creep, stability etc.

The adhesion of the oxide scale and in turn Z_c is also governed by thermal stress (σ_{ox}) [58] given as,

$$\sigma_{ox} = \frac{E_{ox}\Delta T\,(\alpha_{ox} - \alpha_m)}{1 + 2\left(\frac{E_{ox}}{E_m} \times \frac{t_{ox}}{t_m}\right)} \qquad (5)$$

where α_{ox} and α_m are the coefficient of thermal expansion, E_{ox} and E_m are the elastic modulus and t_{ox} and t_m are the thickness of the oxide scale and the substrate metal respectively, ΔT is the temperature difference experienced by the component.

Normally t_{ox} will be negligible compared to t_m simplifying the equation as,

$$\sigma_{ox} = E_{ox}\,\Delta T\,(\alpha_{ox} - \alpha_m) \qquad (6)$$

According to equation (6) the thermal stress is dependent on the differences of thermal expansion coefficient of the oxide scale and the metal substrate. The ratio of the thermal expansion coefficient of the metal substrate and the oxide scale is given in Table 6. Interestingly Fe/Fe_2O_3, Ni/NiO and

Table 6: Thermal expansion coefficient of the oxide and the substrate metal

System	*Oxide coefficient*	*Metal coefficient*	*Ratio*
Fe/FeO	12.2 x 10^{-6}	15.5 x 10^{-6}	1.25
Fe/Fe_2O_3	14.9 x 10^{-6}	15.5 x 10^{-6}	1.03
Ni/NiO	17.1 x 10^{-6}	17.6 x 10^{-6}	1.03
Co/CoO	15.0 x 10^{-6}	14.0 x 10^{-6}	0.93
Cr/Cr_2O_3	7.3 x 10^{-6}	9.5 x 10^{-6}	1.30
Cu/Cu_2O	4.3 x 10^{-6}	18.6 x 10^{-6}	4.32
Cu/CuO	9.3 x 10^{-6}	18.6 x 10^{-6}	2.00

Co/CoO are the system where this ratio is close to 1 giving minimum thermal stress. Thus, surface alloying leading to similar system will result in lower wear rate if the wear regime is in mild oxidational wear.

For a given oxide scale substrate system, the critical thickness for spalling (Z_c) can be increased by,

1. Adding Y, H_f or rare earth elements on the surface [59, 60].
2. Ensuring fine dispersoids near the surface either by internal oxidation or by using mechanically alloyed material [61].
3. Aluminising with noble alloying elements, eg. Pt, Au, Ag, etc. as such addition results in cleaner oxide formation [62-64].

Addition of Y, Hf and rare earth elements increases adhesion of oxide scale, because,

1) Scale grows at scale metal interface into the substrate resulting in mechanical pegging [65].
2) Voids generation at the scale metal interface is prevented by vacancy accommodation [66].
3) Grains become finer. Grain boundry diffusion coefficient increases. These facts promote stress relief by 'Cobble' creep [67].
4) Fine grain scale is produced. Sulphur segregation at the scale metal interface is prevented. This prevents embrittlement at scale-metal interface. It acts as oxygen active dopants [68].

This increase in critical thickness of spalling, resulting in increase of wear resistance is reflected in the work of Wang *et al.* [69] who noted an increase in wear resistance with laser surface alloying of the substrate by CeO_2. Their results illustrated in Fig. 8, which gives, wear rate as function of hardness. Experimental conditions for their work pertain to applied load of 300 N, sliding velocity 0.8 m/s and total sliding distance of 750 m. They used a block on ring configuration with the mating surface being 52100 bearing steel. Clearly a lower wear rate with CeO_2 alloyed surface can be seen. They attributed this observation to refinement of microstructure, strengthening and purifying the grain boundary and improving the morphology and distribution of eutectics. These refinements resulted in more adherent oxide scale, which in turn improved the wear resistance. Further discussion on this is attempted in section 3

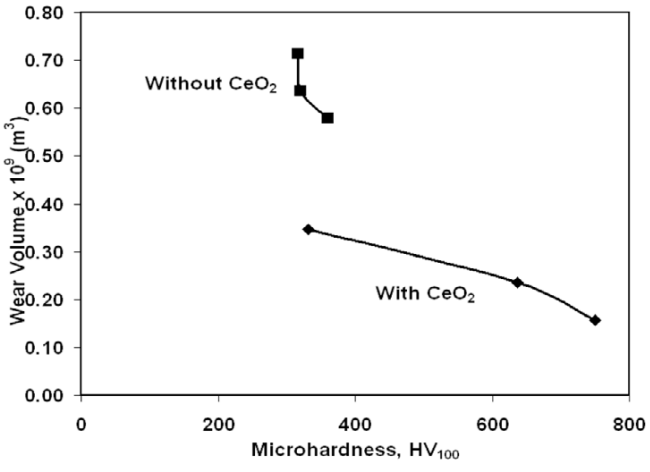

Fig. 8 : The influence of hardness on the wear rate of laser surface alloyed steel (surface alloyed with CeO_2) [69].

Dispersion of small particles improves adhesion by,

1. Dispersoids accumulate at scale-metal interface and block diffusive transport [70].
2. Transport through scale [71].
3. Dispersoids act as nucleation sites and form continuous scale rapidly with finer grains and fewer short circuits path for cataions so that anion diffusion becomes rate controlling [72].

Improvements of wear behaviour of coating obtained using the similar principle is not available in the literature. However, Roy *et al*. [73], using PM-1000 alloy, where adhesion of Al_2O_3 scale is improved by dispersion of fine particles, demonstrated excellent wear properties at elevated temperature. They examined wear and friction behaviour of the dispersion strengthened Ni base alloy PM-1000 under a load of 70 N and sliding speed of 0.25 m/s at various temperature up to 800ºC. Their observation is given in Fig. 9. At all temperature the material experiences a net thickness gain. In this figure, thickness loss is plotted against sliding distance.

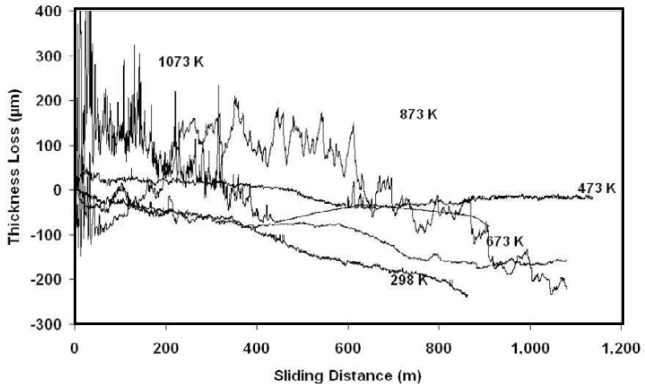

Fig. 9 : Variation of thickness loss with the sliding distance for a dispersion strengthened alloy PM-1000 at various temperatures.

Finally addition of noble metal such as Pt, Au and Ag improves adhesion of oxide scale by,

1. reduction of the stress in the scale by enhanced diffusional creep or through enhanced grain boundary sliding [74].
2. development of pegs underneath the scale [75].

Wells and Dewet and also Eylon *et al.* reported improved wear performances of Pt coated materials [76,77]. The work, due to Wells and Dewets is shown in Fig. 10. In this work, (a) alumna ball, (b) uncoated bearing steel and (c) sputtered ion-plated ball were tested under reciprocating condition at applied load of 10 N, sliding speed of 0.75 m/s, for stroke length of 10 mm. In Fig. 10 the variation of friction coefficient of these materials as function of sliding distance is shown. Their results show not only low friction coefficient of coated bearing steel compared to the substrate and the alumna but also it indicates that friction coefficient remains constant with sliding distances. Presence of platinum allows formation of thin adherent oxide film. This oxide film has very low friction coefficient and wear rate, resulting in improved tribological performances. This is discussed with further details in section 3.

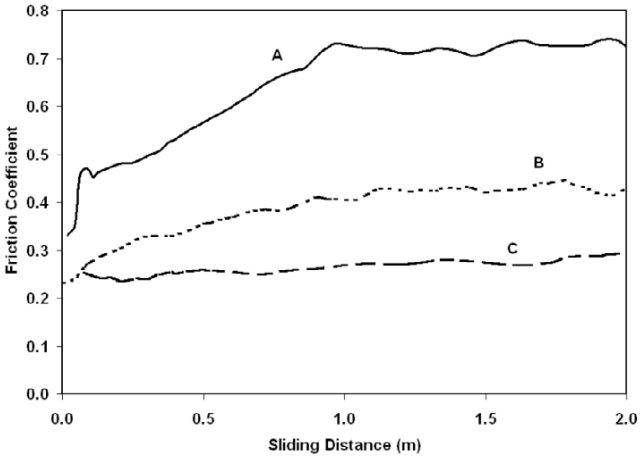

Fig. 10 : The variation of friction coefficient of (a) alumina ball, (b) uncoated bearing steel and (c) sputtered ion Pt coated steel as function of sliding distance [76].

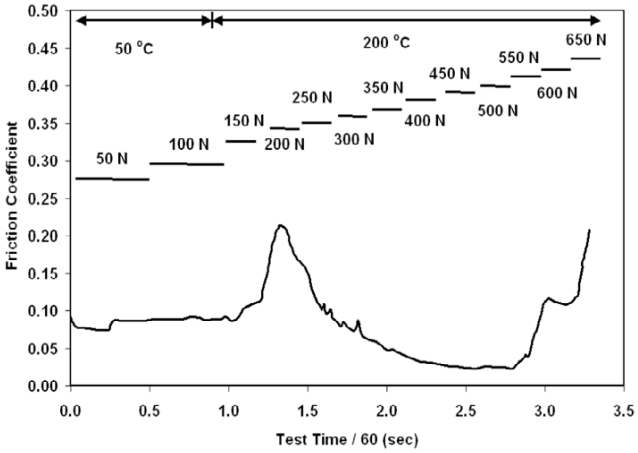

Fig. 11 : The influence of load, test temperature, test time and friction coefficient Al_2O_3/ZrO_2 coated grey cast iron [80].

2.3 Severe oxidational wear

As the applied load and the sliding velocity are increased further, wear mechanism changes from mild oxidational wear to severe oxidational wear. The wear rate in severe oxidational wear regime can be estimated as,

$$W = \frac{f_m \alpha \mu F}{L_{ox}} - \frac{f_m K_{ox} (T_m^{ox} - T_b) F^{1/2} N^{1/2} A_n^{\frac{1}{2}}}{L_{ox} \beta v r_0 H_o^{1/2}} \qquad (7)$$

Where f_m is volume fraction of molten material during sliding, r_o is the radius of the nominal contact area, L_{ox} is the latent heat for fusion per volume of the oxide scale, β is a dimensionless parameters for bulk heating, K_{ox} is the thermal conductivity of the oxide scale, N is the total number of asperities, H_o is the hardness of the oxide scale, T_m^{ox} is the melting temperature of the oxide scale. α, μ, F v and T_b have their usual meaning defined previously.

The wear rate in this regime can be decreased by

1. Increasing K_{ox}
2. Increasing T_m^{ox}
3. Decreasing friction coefficient m, and
4. Decreasing thermal expansion coefficient of the oxide scale.

The values of K_{ox} and T_m^{ox} in this regime are listed in Table 7 [78]. Table 7 indicates the superiority of Cr_2O_3 and Al_2O_3 scale formation for improving wear resistance. Thus, the kind of surface that performs well during mild oxidational wear will do well even under severe oxidational wear. Excellent wear properties of Cr_2O_3 and Al_2O_3 layers are reported by several investigators [79-80]. Fig. 11 represents one such results due to Barbazet *et al.* who investigated the sliding wear of plasma sprayed Al_2O_3-40% ZrO_2 against grey cast iron under a load of 650 N using optimal oscillating wear tester. In this figure the influence of load test temperature on friction coefficient is shown. In this figure, multidimensional friction curve is plotted in two-dimensional form. In this figure results of several interrupted wear test under different condition is compiled. The friction coefficient is strong function of load. It is lower at elevated temperature. In fact at 300ºC for the load of 400 to 550 N the friction coefficient is 0.03 to 0.04. The seizure occurs at 650N. Similarly Roy *et al*. [81] noted reduction of friction coefficient of Cr_2O_3 scale forming Cr_3C_2-25(Ni20Cr) coating, obtained by thermal spraying decreases with increase of test temperature. This coating was subjected to sliding wear at a load of 70 N and at sliding speed of 0.25 m/s. These results given in Fig. 12 can be attributed to high thermal conductivity and high melting temperature of Cr_2O_3 scale.

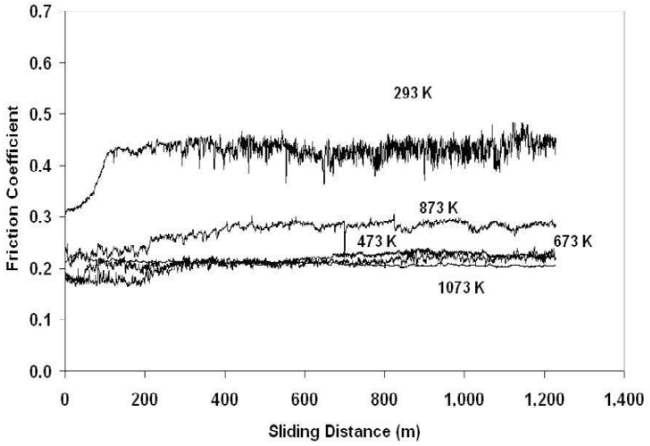

Fig. 12 : The variation of friction coefficient as function of sliding distance for Cr_3C_2-25(Ni20Cr) coating at various test temperature [81].

2.4 Melt wear

At an extreme test condition i.e., at very high load and at very high sliding velocity melt wear becomes important. The wear rate (W) in this regime can be given as,

$$W = \frac{\alpha \mu a F}{L v r_0} - \frac{(T_M - T_o) K_m A_n}{\beta L v r_o} \qquad (8)$$

Where L, T_m and K_m are the latent heat of fusion, melting temperature and thermal conductivity of the wearing material. Other symbols have their usual meaning. The wear rate in this regime can be reduced by

1. reducing μ,
2. reducing L
3. increasing K_m, and
4. increasing T_m.

Thus coating is to be selected having high K_m and T_m and low m and L. The thermal conductivity and melting temperature of various metallic materials are given in Table 8 [78]. The static frictions of various self-mating materials are given in Table 9 [78] and that of various metals against mild steel are given in Table 10 [78]. According to Table 8, W and Mo has good combination of melting point and thermal conductivity. Thus, alloying surface with such material will result in improved performance. Beneficial effect of the surface alloy with W and Mo for wear related use is reported by Hsu and Molion [82]. Similar effect with thermal sprayed Mo is also reported by Okaslo *et al*. [83] and Stachowaik *et al*. [84]. The observation of Okasa *et al*. is shown in Fig. 13 and Fig. 14. In these figures numbers 1,2,3,4, and 5 along X-axis represent counter bodies Ni-P, WC-12%Co, Mo, Al_2O_3-40%TiO_2 and Cr_2O_3 respectively. Different shades correspond to different wearing materials. They conducted wear test with the help of cylinder on cylinder geometry for a combination of two loads (4.9 N and 19.6 N) and two stroke lengths (10 and 56 μm) at a frequency of 7 Hz and for total duration of 200,000 cycles. Figure 13 shows the bar diagram of friction coefficient of various coated system and Fig. 14 represents the wear rate of these systems. The low friction coefficient and wear rate of the cylinder coated by thermally sprayed Mo can be noted. Further comments on this are made in section 3. Cu is one element, which has moderate melting point but very high thermal conductivity. Thus, this metal finds several wear related applications, particularly in bearing materials. Table 9 and Table 10 indicate suitability of

Table 7: Melting point and thermal conductivity of various oxide scale

Oxide scale	*Melting point* (T_m) ^oC	*Thermal conductivity* ($Wm^{-1}K^{-1}$)
Al_2O_3	2050	9.2
Cr_2O_3	2435	8.6
SiO_2	1710	2.0
NiO	1984	
FeO	1367	
CoO	1935	
CuO	1027	

Table 8 : Melting point and thermal conductivity of various pure metals

Metals	*Melting Point* (T_m) ^oC	*Thermal conductivity* ($Wm^{-1}K^{-1}$) *0-100*
Fe	1536	78.2
Al	660.37	238
Si	1412	138.5
Ni	1455	88.5
Cu	1084.8	397
Co	1494	96
Cr	1860	91.3
Mo	2615	137
Ti	1667	21.6
W	3387	174
Zn	418.6	119.5

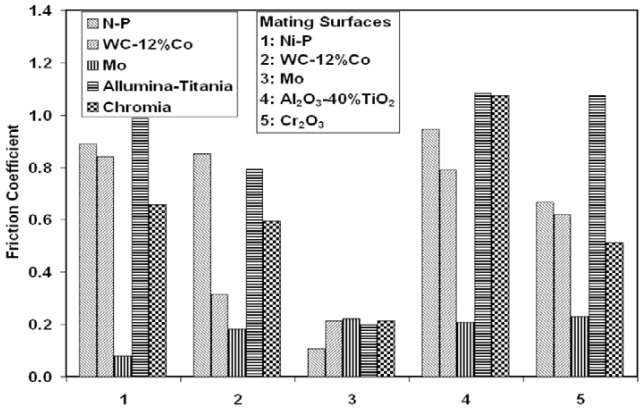

Fig. 13 : Bar diagram showing the friction coefficient of Mo coated steel [83].

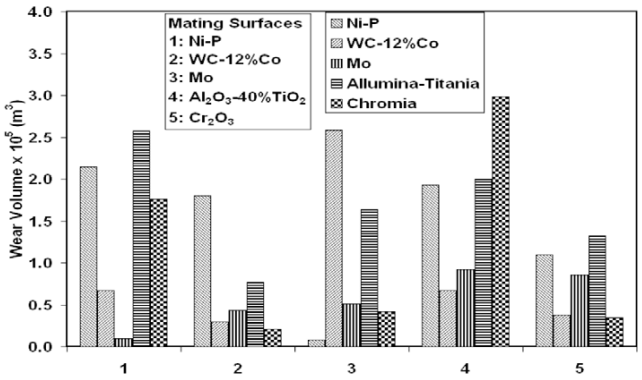

Fig. 14 : Bar diagram showing the wear rate of Mo coated steel [83].

Mo, Co, cast iron, etc., for wear resistance application. Work of Savyer and Blenchat [85] demonstrated the ability of Mo and W to reduce friction coefficient to as low as 0.15 under self-mating condition.

3. Discussion

In this section an attempt will be made to analyse the observation of few investigators in the light of the wear mechanism map. The objective of this section is to justify the understanding of the author on the prevailing wear

Table 9: Static friction of metals in vacuum and in air

Metal	μ_s *in vacuum*	μ_s *in air*
Ag	-	1.4
Al	-	1.3
Co	0.6	0.3
Cr	1.5	0.4
Cu	-	1.3
Fe	1.5	.0
In	-	2
Mg	0.8	0.5
Mo	1.1	0.9
Ni	2.4	0.7
Pb	-	1.3
Pt	4	

Table 10: Static friction of unlubricated metals and alloys on steel

Metals and alloys	*Friction coefficient*
Al	0.6
Al-bronze	0.45
Brass	0.5
Cast iron	0.4
Cr	0.5
Cu	0.8
Cu-Pb	0.2
In	2
Pb	1.5
Mo	0.5
Ni	0.5
Phosphor bronze	0.35
Ag	0.5
Steel	0.8
TiN	0.9

mechanisms of some of the earlier works. The analysis of wear data from this respect is not yet reported in the literature. A thorough quantitative treatment of the wear data is not possible as the test equipments vary over a wide range. Further, not all investigators gave full information about test conditions. Thus a qualitative discussion will be presented.

To begin with, the work of Fu *et al.* [33] will be considered. Using a ball on flat surface, they tested Al 6061 laser surface alloyed with Ni-Cr alloy. The test was conducted for a load of 5 N, sliding velocity of 0.005 m/s. For their test configuration of ball on flat surface the nominal contact area is taken from the expression given in Table 11. The bulk and flash temperature is calculated using equation (2) and equation (4). The relevant thermophysical properties ate taken from ref. [1,78]. The bulk temperature is calculated using the thermophysical properties of Al and flash temperature is calculated using the thermophysical properties of the Ni-Cr alloy. The estimated bulk and flash temperatures are 45ºC and 47ºC respectively. Thus at this low temperature there will be negligible oxidation of Ni-Cr alloy and the wear will be plasticity dominated wear. The melting point of the Ni-Cr alloy is higher than the melting point of Al resulting higher hardness. Further, there is substantial increase in hardness due to laser glazing. Hence, the wear rate in the plasticity-dominated or delamination wear regime is decreased due to increased hardness as can be seen from equation (1).

In the following paragraph few more example will be taken. One important feature of all the example is that all the cases the substrate material is steel. For all the cases the normalised load F_n and the normalised velocity v_n are determined using the equations given below [1].

$$F_n = \frac{F}{A_n H_o} \tag{9}$$

and

$$v_n = \frac{vr}{a} \tag{10}$$

The symbols have their usual meaning. For the purpose of calculation, equation given in Table 11 are employed. Table 11 also gives the equations to be used for estimating the nominal contact area for a number of test configurations. Assuming the thermal diffusivity and hardness of steel to be 9.1×10^{-6} (m^2/s) and 1 GN/m^2 [1] respectively, the normalised load and the normalised velocity are determined. These values for different investigators are listed in Table 12. The results of the test conditions are also reflected in the wear mechanism map (Fig. 15). The work of Budinsky clearly comes

Table 11: Equation employed to compute nominal contact area of various test configuration.

Sl. No.	*Test Configuration*	*Equation for Nominal Contact Area.*	*Meaning of Symbols*
1	Pin on Disc.	$A_n = \pi r^2$	r = radius of the Pin
2	Ball on Flat Surface.	$r = 0.881\{(L\,x\,D)/E\}^{1/3}$ $A_n = \pi r^2$	D = Diameter of the ball
3	Cylinder on Cylinder	$a = 1.075\,(LD/2bE)^{1/2}$ $D = 1/D + 1/D2$ $A_n = 2ab$	D_1 and D_2 are the diameters of the cylinders. b is the length of the cylinder
4	Sphere on Sphere	$r = (3LD/8E)^{1/3}$ $1/D = 1/D_1 + 1/D_2$ $A_n = \pi r^2$	D_1 and D_2 are the diameters of the spheres
5	Block on Ring	$a = 1.075\,(LD/2bE)^{1/2}$ $A_n = 2ab$	D is the diameter of the ring b = width of the block

in the plasticity dominated wear regime as expected by the present author and hence the wear rate improves by diffusion coatings as the surface hardness increases. Further as boronised layer has maximum resistance to softening it has best wear rasistance among various diffusion coatings. The works of other investigators are in an area where all four regimes exist over a small zone. Given the inaccuracies of the wear test condition, the estimation procedure, it can be stated that the work of Well *et al.* is in mild oxidational wear regime, that of Wei and Xue is in severe oxidational wear regime and the work of Okaslo *et al.* is in melt wear regime. In view of the above it is justified that the wear resistance improves by 1) having a layer with higher hardness in plasticity dominated wear regime, 2) improving the adhesion of the oxide scale by adding Pt in the mild oxidational wear regime, 3) having a layer with higher thermal conductivity and higher melting temperature in the severe oxidational wear regime and 4) having a coating with low friction coefficient, high melting temperature and high thermal conductivity in melt wear regime.

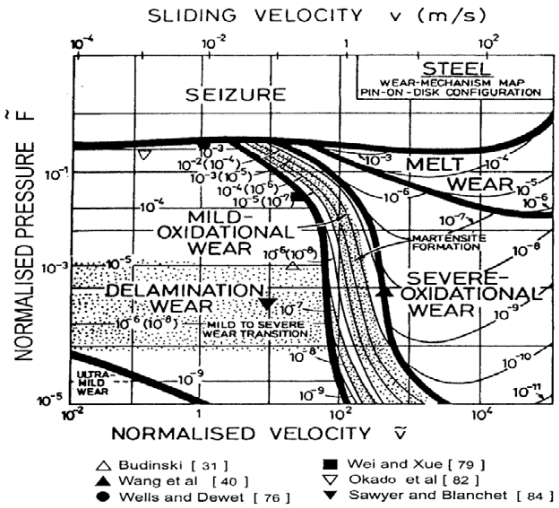

Fig. 15 : The wear mechanism map with the results of present analyses.

Table 12 : Normalised load and normalised velocity of various investigation analysed in this work

Sl. No.	*Name of the Investigator*	*Test Configuration*	*Normalised Load*	*Normalised Velocity*
1	Budinsky [28]	Block on ring	0.00818	83
2	Wang et.al. [38]	Pin on disc	0.00001119	4450
3	Herose et. al. [48]	-	-	-
4	Iswane and Ma [50]	Block on ring	-	-
5	Wang et. Al. [68]	Block on ring	-	-
6	Wells and Dewet [74]	Ball on flat	0.48	1.1181
7	Wei and Xue [77]	Block on ring	0.006	68.87
8	Barbezat et. al. [78]	-	-	-
9	Okaslo et.al. [80]	Cylinder on cylinder	0.098	0.0137
10	Sawyer and Blanchet [82]	Pin on disc	0.0002	22.33

The work of Herose *et al.* [49], Gawne and U.MA [51], Barbezat *et al.* [80] and Wang *et al.* cannot be analyzed in this work. This is primarily due to the fact that sufficient details of their test condition are not available. For example Herose *et al.* [49] did not mention the configuration and dimension of the specimen used in the test. Similarly, Gwane and U.Ma [51] used a configuration for which no standard method exists to calculate the nominal contact area. Further in their configuration no area is constantly wearing out. Wang *et al.* [69] also did not mention the dimension of the ring against which the block is made to slid. From the description of Barbezat *et al.* [80] it is not clear what kind of configuration they have used and what is the dimension of the test specimen.

In short, it is possible to extend or redefine the boundaries of wear mechanism maps as shown in Fig. 1. In general, wear rate in the regime of delamination or plasticity dominated wear will be lower than the wear rate in mild oxidational wear. The wear rate in mild oxidational wear is less than the wear rate of severe oxidational wear and the wear rate of severe oxidational wear is less than the wear rate of melt wear. Under such circumstances, it would be always beneficial to change or alter the boundary by suitably engineering the surfaces and retain the operation of the wearing materials in a regime which exhibit the lower wear rate compared to other possible operating regime. Last but not least, it should be stated that the above discussion is valid for metals and alloys. The discussion changes totally when other materials such as ceramics, polymers or composite materials are considered.

4. Conclusions

- The expression for wear rate in various wear regimes are critically analysed. The important parameters that govern wear rate in each regime are identified. The methods for improving wear rate in each case are suggested. The suggestions are based on modern techniques of surface engineering. The suggested methods are elaborated with published examples and discussion.
- The above work clearly brings out the superiority of formation of Cr_2O_3 and Al_2O_3 layers for wear resistance application. These layers are to perform well for a range of mechanisms of wear.
- The performances of oxide layer can be further improved by taking appropriate measure to increase the adhesion of these coatings.

Acknowledgement

The author is grateful to the director DMRL for his permission to publish this work. The author is also grateful to the reviewer for excellent review work and his suggestions.

References

1. Lim S C and Ashby M F, *Acta Met*, **35** (1987) 11
2. Blomerg A, Olsson M and Hogmark S, *Wear*, **171** (1994) 77
3. Roy M, Ray K K and Sundararajan G, *Metal. And Mater. Trans.*, **32A** (2001) 1431.
4. Hirst W and Lancaster J K, *J. Appl. Phys.* **27** (1956) 1057.
5. Hogmark S, Jacobson S and Larsson M, **Wear**, **246** (2000)20
6. Bunshah R F, Handbook of deposition techniques for films and Coatings, (2nd ed.) Noyes Publications, West wood, New Jersey, USA.
7. Wei Q and Narayan J, *Int. Mater. Review*, **45** (200) 133.
8. Veprek S, *Thin Solid Films*, **317** (1998) 449.
9. Wear Control Handbook, Eds. Peterson M B and Winer W O, New York, (1980).
10. Fundamentals of Friction and Wear, Ed. Regney D.A., Metals Park, Ohio, *ASM*, (1981).
11. Ahmed R and Hadfield M, *Wear*, **230** (1990) 39
12. Roy M, Ch. V Subha Rao, Rao D S and Sundararajan G, S*urface Engineering*, **15** (1999) 129
13. Bozzi A C and B de Mello J D, *Wear*, **233-235** (1999) 575
14. Yinglong W, Yuansheng J and Shizhu W, *Wear*, **128** (1988) 265
15. Roy M and Sundararajan G, Proc. 12th Int. Tribol. Colloquium, Jan, 2000 Stuttgart, Germany, p-1971.
16. Garg D and Dyer P N, *Wear*, **162-164** (1993) 552
17. Voyer J and Marple B R, *Wear*, **225-229** (1999) 135
18. Roy M, Narkhede B E and Paul S N, Proc. Int. Conf. On Industrial Tribol. Dec., 1999 Hyderabad, India, p-215.
19. Wood R J K, Meller B J and Binfield M L, *Wear*, **211** (1997) 70.
20. Bahadur S and Yang C N, *Wear* 196 (1996) 156.
21. Lin P, Deshpandey C, Doerr H J, Bunshah R F, Chopra K L and Vankar V D, *Thin Solid Films,* **153** (1987) 487.
22. Lee K S, Kim Y S, Tosa M, Kasahara A and Yosihara K, *Appl. Surf. Sci.*, **169-170** (2001) 420.
23. Holmberg K and Matthews A, *Coatings Tribology, Tribology Series*, **28**, Elsevier, Amsterdam, (1994).
24. Hiroven J P, Koskien J, Jervis J R and Natasi M, *Surf. Coat. Technol.,* **80** (1996) 139.
25. Hogmark S, Hollman P, Alahelisten A, Hedenqvist P, Wear, **200** (1996) 225.
26. Krishnaraj N, Iyer K J L, Sundaresan S, *Wear* **210** (1997)237
27. Rizvi S A and Khan T I, *Tribol. Intl.*, **32** (1999) 567.
28. Budinski K G, *Wear*, **162-164** (1993) 757.
29. Wang A G and Hutchings I M, *Wear*, **124** (1988)149.
30. Gordienko A I, Ivaskko V V and Bushik S V, *Phy. and Chem. of Materials Treatment,* **23** (1989) 208.
31. Tananko I A, Levchenko A A, Guiva R T, Guiva V A and Sitsevaya E Yu, *Phy. and Chem. of Materials Treatment*, **25** (1991) 529.
32. Sundararajan G, *Scripta. Metal*, **32** (1995) 523.
33. Fu Y, Batchelor A W and Loh N L, *Wear*, **218** (1998) 250.
34. Dingremont N, Bergmann E and Collignon P, *Surf. Coat. Technol.* **72**(3) (1995) 157.
35. Dingremont N, Bergmann E, Collignon P and Michel H, *Surf. Coat. Technol.,* **72**(3) (1995)163
36. Johansson E, Surface modification in tribology, Acta Universitatis Upaliensis Dissertation in Science and Technology, Vol433,1993.ISBN 91-554-3061-6, Paper VII.
37. Jia K and Fischer T E, *Wear*, **200** (1996) 206
38. Wang Y, Jiang S, Wang M and Wang S, Xiao T.D. and Strutt P.R., *Wear*, **237** (2000) 176.
39. Roy M, Pauschitz A, Pollak R and Franek F, *Tribology Int.* **39** (2006) 29.
40. Rebholz C, Leyland A, larour P, Choritidis C, Logotletidis S, and Matthews A, *Surf. Coat. Technol.*, **116-119** (1999) 648.
41. Rebholz C, Leyland A, Schneider D, Schuttrich B, Charitidis C, Logothetidis S and Mathews A., *Thin Solid Films* (in Press)
42. Rebholz C, Schneider J M, Logotletidis S, Matthews A.. *Surf. Coat. Technol.* **112** (1999) 85
43. Quin T F J, Sullivan J L and Rowson D M, *Wear*, **94** (1984)175.
44. Rowson D M and Quinn T F J, *J. Phy. D. Appl. Phys.*, **13** (1980) 209
45. Quin T F J, *Wear*, **216** (1998) 262-275.
46. Malgaord J and Srivastaba V K, *Wear*, **41** (1977) 263.
47. Roy M, Ray K K and Sundararajan G, *Oxid. Metals,* **50** (1999)
48. Kubaschewski O and Hopkins B E, *Oxidation of Metals and Alloys,* Buttersworth London, (1962).
49. Hirose A, Ueda T and Kobayashi K F, *Mater. Sci.and Engg.* **160A** (1993) 143.
50. Tau Y H and Doong J L, *Wear*, **132** (1989) 9.
51. Gawne D T and MA U, *Wear*, **129** (1989) 123.
52. Schmutzler H J, Viefhaus H and Grabke H -J, *Surf. Interface Anal.,* **18** (1992) 581.
53. Dankov P D and Churuev P V, *C.R. Acad. Sci. U.R.S.S.***, 73** (1950) 1221
54. Peters F and Engell H J, *Arch*, Eisenhullenw
55. Cox B, *Progr. Nad. Energy Ser,* **4** (1961) 166
56. Smeltzer W W, *Acta Met.,* **8** (1960) 268
57. Moreau J and Cognet M, *Rev. Metall,* **55** (1958) 1091.
57. Pilling N B and Bedworth R E, *J. Inst. Met.,* **29** (1923) 529
58. Engell H J, Werkstoffe, *Korrosion*, **11** (1960) 147.
59. Hou P Y and Stringer J, *Oxid. Met.,* **38** (1992) 323.
60. Sigler D R, *Oxid. Met.,* **40** (1993) 555.
61. Bennett M J and Haulton P, 'High Temperature Materials for Power Engineering; (ed. E. Bachelet) 189, 1990, Dorlrecht, Kluwer, Academic Publishers.
62. Tatlock G J and Hard T J, *Oxid. Met.*, **22** (1984) 201.
63. Gobel M, Rahmel A and Schertzc M, *Oxid. Met.*, **3-4** (1993) 231
64. Sun J H, Jang H C and Chang E, *Surf. Coat. Technol*., **64** (1994)195
65. Vernon-Perry K D, Crovenor C R M, Needhan N. and English T, *Mater. Sci. Technol.,* **4** (1988) 461
66. Pint B A, *Oxid. Met.,* 48 (1997)303
67. Ramnarayanan T A, Raghavan M and Petkvichuton R, *J. Electrochem. Soc.,* **131** (1984) 923.
68. Forest C and Davidson J H, *Oxid. Metals,* **43** (1995) 479.
69. Wang Y, Kovacevic R, Lia J, *Wear*, **221** (1998) 47-53.
70. Giggin C S and Pettit F S, *Met. Trans.,* **2** (1971) 1071
71. Wood G C and Stott F H, *Mater. Sci. and Technol,* **3** (1987) 517
72. Whittle D P and Stringer J, *Phil. Trans. R. Soc.* (London) **295A** (1980) 304
73. Roy M, Pauschitz A and Franek F, *Tribologie und Schmierungstechnik,* **50** (2003) 40.
74. Fountain J G., Golightly F A, Scott F H and Wood G C, *Oxid. Met.*, **10** (1976) 341
75. Allan I M, Akuezue H C and Whittle D P, *Oxid. Met.,* **14** (1980) 517
76. Wells A and Dewet D J, *Wear,* **127** (1988) 269
77. Eylon D and Belts R K and Fujishro S, *Thin Solid Films*, **73** (1980) 323.
78. Metals Reference Book, e.d. Smithels C.J.. Butterworths. London & Boston, 5th ed. 1976.
79. Wei J and Xue Q, *Wear*, **162-164** (1993) 229.
80. Barbezat G, Nicoll A R and Sickinger A, *Wear*, **162-164** (1993) 529-537.
81. Roy M, Pauschitz A and Franek F, Proc. Int. Corrosion Congress. Sept.,2002, Granada, Spain.
82. Hsu M J and Molians P A, *Wear*, **132** (1989) 123
83. Okado J, Shima M, Mccoll I R, Watertions R B, Osegava T H and Kasaya M, *Wear*, **225-229** (1999) 749.
84. Stachowiak G W, Stachowiak G D and Batchelor A W, *Wear* **178** (1994) 69.
85. Sawyer W G and Blanchal T A, *Wear*, **225-229** (1994) 581.